

# Wave & current-induced progressive liquefaction in loosely deposited seabed



Guoxiang Yang<sup>a</sup>, Jianhong Ye<sup>a,b,\*</sup>

<sup>a</sup> Department of Civil Engineering, School of Engineering and Technology, China University of Geosciences, Beijing 100083, China

<sup>b</sup> State Key Laboratory of Geomechanics and Geotechnical Engineering, Institute of Rock and Soil Mechanics Chinese Academy of Sciences, Wuhan 430071, China

## ARTICLE INFO

### Keywords:

Pore pressure build up  
Progressive residual liquefaction  
Loosely deposited seabed floor  
Wave & current  
Pastor-Zienkiewicz Mark III  
FSSI-CAS 2D

## ABSTRACT

Quaternary newly deposited loose seabed soil widely distributes in offshore area in the world. Wave-induced residual liquefaction in loose seabed floor brings great risk to the stability of offshore structures in extreme climate. Understanding of the characteristics of wave-induced residual liquefaction in loose seabed is meaningful for engineers involved in design of offshore structures. In this study, wave & current-induced residual liquefaction in loose seabed floor is investigated deeply and comprehensively adopting a validated integrated numerical model. The time history of wave & current-induced pore pressure, effective stress, shear stress, lateral pressure coefficient  $K_0$ , stress angle, displacement of seabed soil are all quantitatively demonstrated. The variation process of progressive liquefaction, stress path, as well as stress-strain relation also are illustrated in detail. The classic effective stress principle has been modified to describe the nonlinear phenomenon that the reduction rate of vertical effective stress  $\sigma'_z$  is faster than that of horizontal effective stress  $\sigma'_x$  and  $\sigma'_y$  accompanying residual pore pressure build up. It is shown that the integrated numerical model FSSI-CAS 2D incorporating PZIII soil model can effectively and precisely capture a series of nonlinear dynamic response characteristics of loose seabed floor under wave & current loading. The computational results further confirm the wave & current-induced liquefaction in loose seabed soil is progressively downward, initiating at seabed surface. Besides, it is found that three physical processes, including vertical distribution of oscillatory pore pressure, time history of stress angle as well as lateral pressure coefficient  $K_0$  could be taken as indirect indicator to judge the occurrence of wave-induced residual liquefaction, and predict the residual liquefaction depth in loose seabed. It is also found that the progressive liquefaction process is significantly affected by wave height, permeability and saturation of seabed soil.

## 1. Introduction

In recent 20 years, a great number of marine structures, such as breakwater, are widely constructed in offshore area. The stability of offshore marine structures under ocean wave loading is the main concern of ocean engineers involved in design. Understanding of the dynamic response characteristics of seabed foundation to ocean wave is a key factor when evaluating the stability of offshore structures during their service period.

In offshore environment, newly deposited Quaternary seabed soil is widely distributed, for example, the loose silty soil in the zone of estuary of Yellow River in China. Actually, a great number of offshore structures have been built on Quaternary sediments. The particle arrangement of Quaternary seabed soil generally is relatively loose, far from being very dense. Under cyclic ocean wave loading (magnitude

should be greater than a critical value), soil particles re-arrange their relative positions to a more dense status, accompanying a pore water drainage process. In this process, pore water pressure builds up, making soil liquefy, or soften. Therefore, it is very dangerous to build a marine structure on newly deposited Quaternary seabed floors. In this study, the wave-induced dynamic response characteristics of newly deposited seabed soil, rather than very dense seabed soil (elastic deformation is dominant) is exactly the focus.

On the problem of wave-seabed interaction, there have been a series of investigation in previous literatures. Analytical solution was first proposed to study the wave-induced dynamics of seabed soil based on Biot's theory. Due to the limitation of analytical methods, seabed soil must be very dense soil in which elastic deformation is dominant under wave loading. Dense seabed soil could be infinite (Yamamoto et al., 1978; Madsen, 1978) or finite (Hsu and Jeng, 1994; Jeng and

\* Corresponding author.

E-mail address: [Yejianhongcas@gmail.com](mailto:Yejianhongcas@gmail.com) (J. Ye).

Hsu, 1996) in depth; also it could be isotropic or anisotropic, one layer or multi-layers (Zhou et al., 2013). The wave adopted in these analytical solutions were all based on Stokes wave theory. It could be progressive wave, standing wave or short-crested wave (Hsu and Jeng, 1994). The governing equation for seabed soil could be consolidation equation, 'u-p' approximation, and 'u-w' equation (Liao et al., 2015a). Generally, uncoupled method was adopted in the above mentioned analytical solutions. There was no feedback from seabed soil to ocean wave when seabed soil responding to wave loading. Fortunately, there were also a few analytical solutions were proposed for wave-seabed interaction (Lee et al., 2002), in which the continuity of pore pressure and fluid exchange on seabed surface were considered. However, the existence of offshore structures on seabed floor could not be taken into consideration.

Beside analytical solution, numerical solution is also a useful tool to investigate the wave-induced dynamics of seabed soil. In the early stage, elastic soil model was used to describe the dynamics of seabed soil in most of previous literature (Jeng, 2003), assuming seabed soil was in very dense state. Naturally, very dense seabed soil rarely exists in offshore area. Newly deposited seabed soil exactly should be concerned by ocean engineers involved in structure design. Due to the flexibility of numerical model, it is possible to describe the nonlinear behavior of loose seabed soil adopting some advanced soil models. In previous literature, there were basically two types of method widely used to study the pore pressure response in loose seabed soil to wave loading. The first method was based on the following governing equation:

$$\frac{\partial p}{\partial t} = c_v \nabla^2 p + f \quad (1)$$

where  $p$  was the pore pressure in loose seabed,  $c_v$  was the consolidation coefficient.  $f$  was a source term to describe the mechanism of pore pressure build up in loose seabed soil under wave loading. It was expressed by Seed et al. (1976) and Seed and Rahman (1978) as

$$f = \frac{\sigma'_{z0}}{N_L} \frac{1}{T}, \quad (2)$$

where  $\sigma'_{z0}$  was the initial vertical effective stress,  $T$  was the period of wave loading,  $N_L$  was the cyclic number of loading making loose soil reaching liquefaction. Generally, it was directly related to the shear stress ratio  $\tau/\sigma'_{z0}$ , and could be determined by fitting and regressing the laboratory test data:

$$N_L = \left( \frac{1}{a} \frac{\tau}{\sigma'_{z0}} \right)^{\frac{1}{b}}. \quad (3)$$

in which  $\tau$  was the amplitude of shear stress;  $a$  and  $b$  were the fitting coefficients. Generally, they were dependent on the relative density of soil  $D_r$ .

Some researchers have successfully obtained the closed form solution of Eq. (1) using analytical method for the problem of pore pressure build up in loose seabed soil under ocean wave loading (Rahman and Jaber, 1986; Cheng et al., 2001). However, their solutions basically were only limited to one dimensional cases. For 2D or 3D cases, it is better to use numerical method to solve (Li and Jeng, 2008). In most previous investigation regardless of analytical or numerical solution, the amplitude of shear stress in seabed, which will be used in Eq. (1), was determined based on poro-elastic theory, assuming seabed soil was being very dense status. Obviously, this assumption was seriously contradictory with the mechanism of pore pressure build up in loose seabed soil. There were two reasons for this contradiction: (1) elastic deformation was not dominant deformation in loose seabed soil under ocean wave loading; (2) shear stress in loose seabed should be gradually reducing in the process of pore pressure build up; when loose seabed soil becoming liquefied, shear stress in soil actually become zero finally (Ye and Wang, 2015). This dynamic

response mechanism can not be effectively described by poro-elastic theory. The amplitude of wave-induced shear stress in seabed determined by poro-elastic theory is a constant, rather than a reducing value. As a result, the action of ocean wave in loose seabed is highly overestimated if shear stress is determined by poro-elastic theory; and pore pressure ratio  $r_u = p_{excess}/\sigma'_{z0}$  in sandy seabed soil could be much greater than 1.0, maybe to 3.0-5.0 (Jeng and Zhao, 2015), (of course,  $r_u$  could be a little greater than 1.0 in cohesive soil). Obviously, this poro-elastic theory based method is insufficient to study the dynamics characteristics of loose seabed soil to ocean wave. Until recently, there are still several similar works published adopting poro-elastic theory to determine wave-induced shear stress in loose seabed, and further estimating the pore pressure build up process.

The second method is that elasto-plastic constitutive soil model is used to describe the nonlinear behaviour of loose seabed soil under wave loading. Sassa et al. (2001) proposed an effective model to study the pore pressure build up in loose seabed soil under wave loading based on the concept of two-layer fluid system and moving boundary. A simplified constitutive equation  $\frac{dv^p}{dt} = \beta \left[ v_\infty^p \left( \frac{\tau}{\sigma'_z} \right) - v^p \right]$  was used to describe the plastic volume strain rate of loose seabed soil under cyclic loading, in which  $v^p$  was plastic volume strain,  $\infty$  represented the ultimate state. Even though the above constitutive equation was simple, the predicted results of pore pressure build up agreed with test data very well. However, effective stress in loose seabed could not be determined by this model; After that, several similar works have also been conducted by Liu et al. (2009), Xu and Dong (2011) and Liao et al. (2015b) to extend Sassa's model to two dimension and random ocean wave case. Oka et al. (1994) developed a FEM model incorporating a nonlinear elasto-plastic constitutive soil model to study the dynamics of loose seabed to linear ocean wave adopting one dimension case. Their work played an important pushing role in this field. Similar work was also performed by Lu and Cui (2004). After that, Dunn et al. (2006) investigated the wave-induced liquefaction in loose seabed around a buried pipelines under linear progressive water wave, adopting a widely verified advanced soil model Pastor-Zienkiewicz Model Mark-III (PZIII) proposed by Zienkiewicz and Mroz (1984) and Pastor et al. (1990). Ou (2009) and Jeng and Ou (2010) further extended PZIII model from 2D to 3D. Their work promoted the investigation of wave-induced liquefaction in loose seabed to a new level. However, their results were insufficient to fully recognize and understand the dynamic response characteristics of loose seabed to ocean wave comprehensively and deeply. The purpose of this study is to further explore and reveal the dynamic response characteristics of loose seabed to ocean wave in the same framework, letting us more deeply understand the mechanism of wave-induced liquefaction in loose seabed.

Some laboratory wave flume tests have been conducted for this problem (Chang et al., 2007; Sassa and Sekiguchi, 1999; Sumer et al., 2006; Kirca et al., 2013; Summer et al., 2010). Their experimental results played very important role in improving our recognition on wave-induced liquefaction in loose seabed soil. However, only the result of pore pressure, displacement and some qualitative phenomena have been observed. Presently, it is short of numerical result to comprehensively and deeply understand the response characteristics of loose seabed foundation to ocean progressive wave & current. In this study, taking an integrated numerical model FSSI-CAS 2D (Ye et al., 2013) as the tool, the wave & current-induced liquefaction mechanism of newly deposited loose seabed soil is investigated. The advanced soil constitutive model—Pastor-Zienkiewicz Mark III (PZIII) proposed by Pastor et al. (1990) is used to describe the complicated nonlinear dynamic behaviour of loose seabed soil. The variation of void ratio  $e$ , and corresponding permeability  $k$  of soil is considered in this computation. Additionally, the stiffness matrix [K] highly depending on effective stress state is also updated using current effective stress in

computation, to fully consider the nonlinearity of dynamics of loose seabed to ocean wave. Results indicate that FSSI-CAS 2D incorporating PZIII model has effectively and precisely captured a series of nonlinear dynamic response characteristics of loose seabed to progressive ocean wave.

## 2. Numerical model and constitutive model

Dynamic Biot's equation known as “ $u - p$ ” approximation proposed by Zienkiewicz et al. (1980) are used to govern the dynamic response of the porous seabed soil under seismic wave loading:

$$\frac{\partial \sigma'_x}{\partial x} + \frac{\partial \tau_{xz}}{\partial z} = -\frac{\partial p_s}{\partial x} + \rho \frac{\partial^2 u_s}{\partial t^2}, \quad (4)$$

$$\frac{\partial \tau_{xz}}{\partial x} + \frac{\partial \sigma'_z}{\partial z} + \rho g = -\frac{\partial p_s}{\partial z} + \rho \frac{\partial^2 w_s}{\partial t^2}, \quad (5)$$

$$k \nabla^2 p_s - \gamma_w n \beta \frac{\partial p_s}{\partial t} + k \rho_f \frac{\partial^2 \epsilon_v}{\partial t^2} = \gamma_w \frac{\partial \epsilon_v}{\partial t}, \quad (6)$$

where  $(u_s, w_s)$  = the soil displacements in the horizontal and vertical directions, respectively;  $n$  = soil porosity;  $\sigma'_x$  and  $\sigma'_z$  = effective normal stresses in the horizontal and vertical directions, respectively;  $\tau_{xz}$  = shear stress;  $p_s$  = the pore water pressure;  $\rho = \rho_f n + \rho_s (1 - n)$  is the average density of porous seabed;  $\rho_f$  = the fluid density;  $\rho_s$  = solid density;  $k$  = the Darcy's permeability;  $g$  = the gravitational acceleration,  $\gamma_w$  is unit weight of water and  $\epsilon_v$  is the volumetric strain. In Eq. (6), the compressibility of pore fluid ( $\beta$ ) and the volumetric strain ( $\epsilon_v$ ) are defined as

$$\beta = \left( \frac{1}{K_f} + \frac{1 - S_r}{p_{w0}} \right), \quad \text{and} \quad \epsilon_v = \frac{\partial u_s}{\partial x} + \frac{\partial w_s}{\partial z}, \quad (7)$$

where  $S_r$  = the degree of saturation of seabed,  $p_{w0}$  = the absolute static pressure and  $K_f$  = the bulk modulus of pore water, generally,  $K_f = 2.24 \times 10^9$  N/m<sup>2</sup>. Here, the compressibility of pore fluid  $\beta$  is taken to consider the unsaturation of seabed soil, which is only applicable for nearly saturated soil. In fact, the saturation of seabed soil in offshore area generally is greater than 90%, which is in the application range of  $\beta$ .

FE method is used to solve the above governing Eqs. (4) to (6), and Generalized Newmark scheme (implicit scheme) is adopted to calculate time integration when solving the above governing equations (Chan, 1988). For the problem of Fluid-Structure-Seabed Interaction (FSSI), a coupled numerical model FSSI-CAS 2D was developed by Ye (2012a). In FSSI-CAS 2D, the Volume Average Reynold Average Navier Stokes (VARANS) equation (Hsu et al., 2002) governs wave motion and porous flow in porous seabed. The above dynamic Biot's equation governs the dynamic behaviour of offshore structure and its seabed foundation. A coupled algorithm is developed to couple VARANS equation and Biot's dynamics equation together. More detailed information about the coupled model can be found in Ye et al. (2013), Ye (2012a) and Zienkiewicz et al. (1999).

Void ratio  $e$  and related Darcy's permeability  $k$  of soil variate based on the deformation characteristics of granular materials. In the most previous investigation, this variation process generally was not considered based on small deformation assumption, namely, void ratio  $e$  and permeability  $k$  kept constant. In this study, standing wave-induced variation of void ratio of seabed soil is considered following formulation  $e_{n+1} = (1 + e_n) \exp\left(\frac{\Delta p}{Q} + \Delta \epsilon_{vs}\right) - 1$ , which is established from the prospect of large deformation, where  $n$  stands for  $n^{\text{th}}$  time step,  $\Delta p$  is the incremental pore pressure,  $\Delta \epsilon_{vs}$  is the incremental volumetric strain of soil, and  $Q = 1/\beta$  is the compressibility of pore water. Correspondingly, permeability of seabed soil  $k$  variates following  $k = C_f \frac{e^3}{1+e}$ , where  $C_f$  is an empirical coefficient, determined by  $C_f = k_0 \frac{1+e_0}{e_0^3}$  (Miyamoto et al., 2004), where  $e_0$  is the initial void ratio.

Additionally, the hydrostatic water pressure, as well as hydrodynamic pressure acting on seabed floor, as the boundary values in FE computation, is variable based on the wave-induced deformation of seabed floor. Under wave loading, the void ratio of loose seabed soil would reduce, leading to the subsidence of seabed surface. As a result, the hydrostatic pressure acting on seabed surface would change significantly, especially in the cases involving large deformation.

In FSSI-CAS 2D, an excellent soil model Pastor-Zienkiewicz-Mark III (PZIII) proposed by Pastor et al. (1990) is adopted to describe the dynamic behavior of loose seabed soil under seismic wave loading. The reliability of PZIII has been validated by a series of laboratory tests involving monotonic and cyclic loading, especially by the centrifuge tests in VELACS project (Zienkiewicz et al., 1999). This model is one of the heritages of Olek Zienkiewicz (Pastor et al., 2011).

## 3. Verification

The validity and reliability of the developed semi-coupled numerical model FSSI-CAS 2D have been widely verified by Ye (2012a). Adopting the analytical solution proposed by Hsu and Jeng (1994), and a series of laboratory wave flume tests conducted by Lu (2005) for regular wave and cnoidal wave, Tsai and Lee (1995) for standing wave, Mizutani et al. (1998) for submerged breakwater, and Mostafa et al. (1999) for composite breakwater, the developed semi-coupled numerical model FSSI-CAS 2D was used to reproduce the dynamic response of elastic seabed foundation and/or breakwater. The good agreement between the predicted numerical results and the corresponding experimental data indicated that FSSI-CAS 2D was a highly reliable for the problem of Wave-seabed-Structure Interaction. Furthermore, the validity and reliability of FSSI-CAS 2D for the problem of wave-loose seabed soil interaction is also verified by a wave flume test (Teh et al., 2003) and a geotechnical centrifuge test (Sassa and Sekiguchi, 1999). More detailed information about the verification work can be found in Ye (2012a); and related works have been published in (Ye et al., 2013).

## 4. Computational domain, boundary conditions and hydrodynamic loading

A flat seabed with 400 m long and 20 m thick is chosen as the computational domain (Noted:  $z = 0$  is set at the bottom of domain; and  $x = 0$  is set at the left lateral side). The mesh size in horizontal is 1 m; and it is 0.5 m in vertical. Totally 12000 4-nodes FE elements are generated. The following boundary conditions are applied in computation: First, the bottom of seabed foundation is impermeable. Second, the two lateral sides are fixed only in horizontal. Third, hydrostatic pressure is applied on the surface of seabed. In each time step, the hydrostatic pressure acting on seabed floor, which is as the boundary values on seabed surface, is updated as  $p_s = \rho g d_0 + \rho g s_v$ , where  $d_0$  is the initial water depth.  $s_v$  is the residual vertical subsidence plus the oscillatory vertical displacement of points on seabed floor resulting from wave loading. Forth, progressive wave-current-induced dynamic pressure acting on the seabed is also applied accompanying hydrostatic pressure, expressed as third-order formulation (first explicitly formulated by (Ye and Jeng, 2012)).

$$P_b(x, t) = \frac{\rho_f g H}{2 \cosh \lambda d} \left[ 1 - \frac{\omega_2 \lambda^2 H^2}{2(U_0 \lambda - \omega_0)} \right] \cos(\lambda x - \omega t) + \frac{3\rho_f H^2}{8} \left\{ \frac{\omega_0(\omega_0 - U_0 \lambda)}{2 \sinh^4(\lambda d)} - \frac{g \lambda}{3 \sinh 2\lambda d} \right\} \cos 2(\lambda x - \omega t) + \frac{3\rho_f \lambda H^3 \omega_0(\omega_0 - U_0 \lambda)}{512} \frac{(9 - 4 \sinh^2(\lambda d))}{\sinh^7 \lambda d} \cos 3(\lambda x - \omega t) \quad (8)$$

where  $\rho_f$  is density of sea water,  $g$  is gravity,  $H$  is wave height,  $\lambda = L/2\pi$  is wave number, where  $L$  is wave length,  $\omega = T/2\pi$  is angle frequency.  $U_0$  is current velocity. Here,  $d = d_0 + s_v$  is the immediate water depth.  $\rho_f$  is the density of sea water. When there is no current in

**Table 1**  
Model parameters of loose seabed soil for PZIII in analysis.

Item	Nevada dense sand	Unit
$K_{evo}$	2,000	[kPa]
$G_{eso}$	2,600	[kPa]
$p'_0$	4	[kPa]
$M_g$	1.32	–
$M_f$	1.3	–
$\alpha_f$	0.45	–
$\alpha_g$	0.45	–
$\beta_0$	4.2	–
$\beta_1$	0.2	–
$H_0$	750	–
$H_{UV}$	40,000	[kPa]
$\gamma_u$	2.0	–
$\gamma_{DM}$	4.0	–

wave ( $U_0 = 0$  m/s), the above third-order solution can be reduced to the classic form of the solution of third-order non-linear wave. When applying the hydrostatic and hydrodynamic water pressure on seabed floor, the effective stresses on seabed surface must be guaranteed as 0.

The parameters of loosely deposited seabed soil for PZIII constitutive model are listed in Table 1, which were determined by Zienkiewicz et al. (1999) for Nevada sand ( $D_r = 60\%$ ) when attending the VELACS project hosted by American National Science Foundation (NSF). Actually, these model parameters for PZIII can be determined by conducting a series of laboratory tests for real soils sampled from offshore seabed floor. The initial void ratio  $e$ , saturation of seabed soil used in computation is 0.333, and 98%, respectively. Correspondingly, the initial permeability of seabed soil is  $1.0 \times 10^{-5}$  m/s. The initial water depth  $d_0$  of sea water over seabed floor is 10 m. Wave height and wave period is set as 1.5 m and 8.0 s, respectively. Current velocity  $U_0 = 0.5$  m/s (co-flow). Computational results on symmetrical lines  $x = 200$  m are recorded, taking as representatives to demonstrate the dynamics of loose seabed soil to progressive wave and current.

## 5. Results

In offshore environment, the seabed soil generally has experiences a long-term consolidation process under hydrostatic pressure. There is no any excess pore pressure in seabed soil before ocean wave loading being applied. This initial consolidation state should be first determined (Ye, 2012b). Then, it is taken as the initial condition for the followed dynamic analysis. It is noted that the compression is taken as positive value.

### 5.1. Effective stresses and pore pressure

Effective stresses and pore pressure are two important indicators to understand the dynamic response characteristics of loose seabed floor to progressive ocean wave & current. Fig. 1 shows the time history of wave & current-induced excess pore pressure and effective stress at three typical buried depths ( $z = 18.5$  m is near to seabed mud line,  $z = 10$  m is at the middle depth, and  $z = 2$  m is near to seabed bottom) in loose seabed floor. It is observed that pore pressure builds up under ocean wave & current loading at any depth in loose seabed floor. There are two components of wave & current-induced pore pressure: residual component and oscillatory component. The amplitude of oscillatory pore pressure is negatively related to buried depth; and the time for residual pore pressure to reach its peak value is positively related to buried depth. However, the magnitude of residual pore pressure in lower seabed is significantly greater than that in upper seabed. Wave & current-induced residual pore pressure can not build up unlimitedly. After its peak value being reach, residual pore pressure basically keeps its state. Actually, it is accompanied by a pore pressure

dissipation process, which is not obvious until  $t = 800$  s.

Corresponding to the build up of residual pore pressure, effective stress in loose seabed floor reduces from its initial consolidation state. When effective stress approaching zero stress state, seabed soil will lost its shear strength and bearing capacity, resulting in collapse of offshore structures if it is as a foundation. As illustrated in Fig. 1, the mean effective stress  $I_1/3$  at  $z = 18.5$  m approaches the zero stress state at about  $t = 150$  s, becoming partially liquefied. At  $t = 300$  s,  $I_1/3$  becomes zero. It means that the seabed soil at  $z = 18.5$  m becomes fully liquefied. In the process of effective stress reducing, the amplitude of shear stress also reduces. When seabed soil at  $z = 18.5$  m becoming fully liquefied, wave & current-induced shear stress also becomes zero due to the fact that a fully liquefied soil behaves like a kind of heavy fluid. As we know, fluid has not ability to transmit shear stress in nature. Our model can clearly captures this phenomenon. It is also observed that  $I_1/3$  at  $z = 10$  m always can not reach fully liquefied state. However, the ratio of the reduction of  $I_1/3$  to its initial value at  $z = 10$  m is greater than 0.9. Therefore, the seabed soil at  $z = 10$  m actually has been become partially liquefied at about  $t = 300$  s. At  $z = 2$  m, the effective stress is far away from the zero stress state. It is not liquefied under wave & current loading until  $t = 800$  s.

In static state, lateral pressure coefficient  $K_0 = \frac{\sigma'_x}{\sigma'_z}$  generally is 0.5 in homogeneous seabed soil. Under dynamic state, this coefficient is variable. Fig. 2 demonstrates the variation process of  $K_0$  at  $z = 18.5$  m under wave & current loading. For dense seabed soil, recoverable elastic deformation is the dominant deformation under wave loading. As a result,  $K_0$  regularly vibrates around 0.5, like harmonic function sine or cosine. However, the variation of  $K_0$  in loosely deposited seabed floor is significantly different. There are also residual and oscillatory component for  $K_0$  in loose seabed. The amplitude of oscillatory component of  $K_0$  is much greater than that in dense seabed. Additionally, the residual component of  $K_0$  gradually increases from its initial value 0.5 until to  $t = 300$  s under wave & current loading. It is also interesting to find that the residual component of  $K_0$  basically keeps stable after  $t = 300$  s; and the amplitude of oscillatory component of  $K_0$  after  $t = 300$  s suddenly becomes significantly greater than that before  $t = 300$  s. Combining the analysis related to Fig. 1, it has been known that the loose seabed soil at  $z = 18.5$  m becomes fully liquefied. Here, it may be concluded that the phenomenon showing stable residual component of  $K_0$  after increasing, and significant increase of the amplitude of oscillatory component of  $K_0$  could be used as an indirect indicator to judge the occurrence of full liquefaction.

As analyzed above, the residual component of  $K_0$  gradually increases from initial value 0.5 in loose seabed floor before occurring full liquefaction. It is indicated that the reduction of effective stress  $\sigma'_x$  and  $\sigma'_z$  is not synchronous accompanying residual pore pressure build up. The reduction speed of  $\sigma'_z$  is greater than that of  $\sigma'_x$ . This phenomenon may be contradictory with the typical effective stress principle  $\sigma'_{ij} = \sigma_{ij} - Ip$ . Effective stress principle presents that effective stress of soil should reduce synchronously accompanying residual pore pressure build up. Therefore, typical effective stress principle should be modified to describe this kind of nonlinear phenomenon as:

$$\sigma'_{ij} = \sigma_{ij} - \begin{Bmatrix} \alpha_x \\ \alpha_y \\ \alpha_z \end{Bmatrix} \delta_{ij} p \quad (9)$$

where  $(\alpha_x, \alpha_y, \alpha_z)^T$  is defined as pore pressure coefficient. In order to determine  $\alpha_x, \alpha_y, \alpha_z$ , the total stress  $\sigma_{ij}$  must be estimated. Due to the fact the total stress frequently is only related to external loading condition, basically has no relationship with soil state. Therefore, total stress in loose seabed floor can be estimated adopting the elastic solution. The determined values of  $\alpha_x, \alpha_y, \alpha_z$  are illustrated in Fig. 3. It is observed that  $\alpha_z$  is indeed greater than  $\alpha_x$  and  $\alpha_y$ , indicating that vertical effective stress  $\sigma'_z$  reducing much faster than that of horizontal effective stress  $\sigma'_x$  and  $\sigma'_y$ , accompanying residual pore pressure build up. Additionally,  $\alpha_x$  and  $\alpha_y$  are basically the same; and  $\alpha_z$  will not exceed

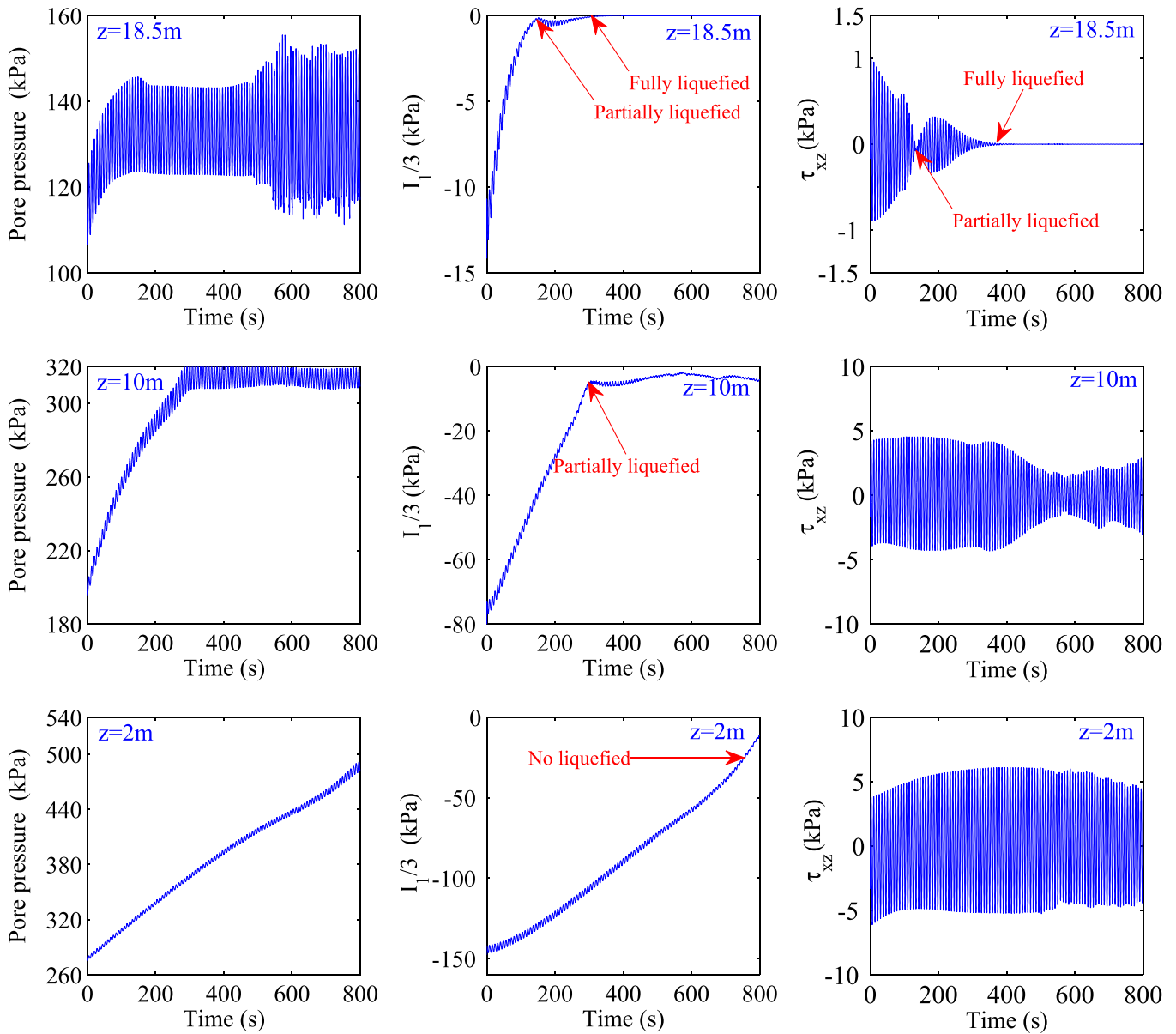


Fig. 1. Time history of wave & current-induced pore pressure and mean effective stress  $I_1/3$  at three typical buried depths in loose seabed floor.

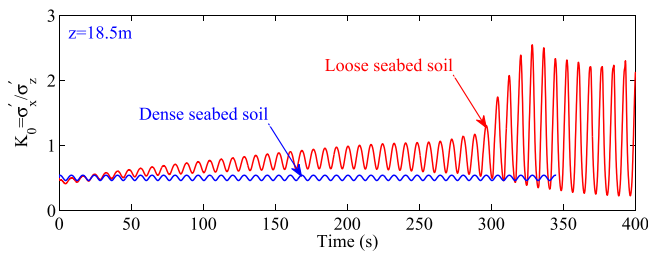


Fig. 2. Variation of wave & current-induced lateral pressure coefficient  $K_0$  in upper seabed floor.

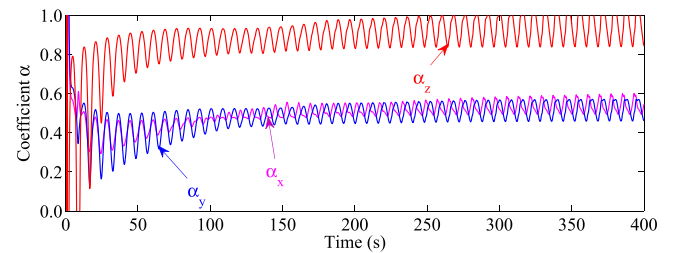


Fig. 3. Variation of pore pressure coefficient  $\alpha_x$ ,  $\alpha_y$  and  $\alpha_z$ .

1.0 in the whole process of wave & current loading. It is noted that the value of  $\alpha_x$ ,  $\alpha_y$ ,  $\alpha_z$  may be different from case to case. It needs more research works in the future.

Stress angle is another physical parameter to study the dynamics characteristics of loose seabed floor to wave & current. Stress angle is defined based on the conception of Mohr-Coulomb criteria as:

$$\theta_{MC} = \arctan \left\{ \frac{\frac{\sigma'_1 - \sigma'_3}{2}}{\frac{c}{\tan \phi} + \frac{\sigma'_1 + \sigma'_3}{2}} \right\} \quad (10)$$

where  $\theta_{MC}$  is stress angle,  $c$  and  $\phi$  are the cohesion and internal friction angle of seabed soil.  $\sigma'_1$  and  $\sigma'_3$  are the maximum and minimum principle stresses.

Fig. 4 illustrates the time history of wave & current-induced stress

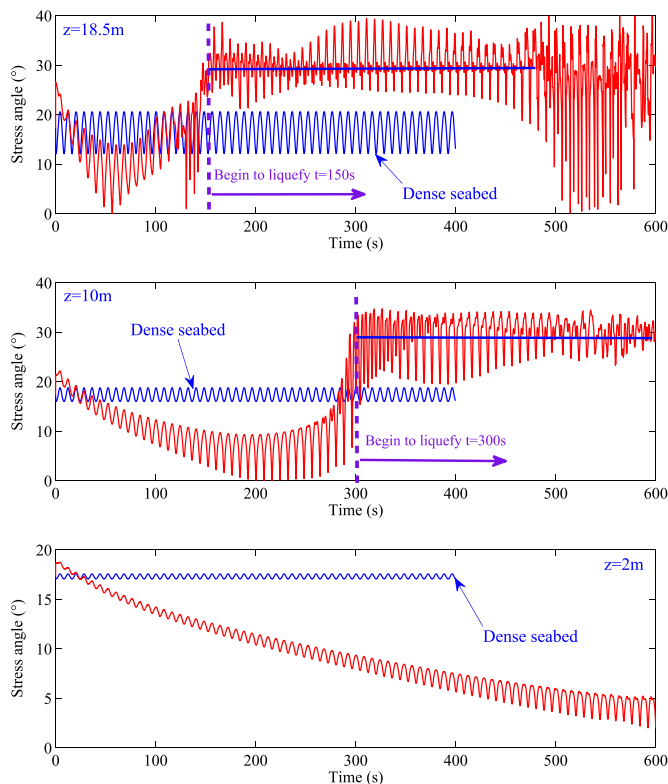


**Fig. 4.** Time history of wave & current-induced stress angle variation at three typical buried depths in loose seabed floor.

angle variation at three typical buried depths in loose seabed floor. As a comparison, the variation of stress angle in very dense elastic seabed floor under the same conditions is also plotted. For dense seabed floor, stress angle only varies periodically around its initial value. However, stress angle in loose seabed floor generally reduces at early stage, and then it gradually increases until the seabed soil become partially or fully liquefied at a buried depth. After that, the residual stress angle basically keep stable. In Fig. 4, it is observed that the time for residual stress angle from increasing to keeping stable at position  $z = 18.5$  m is  $t = 150$  s. Meanwhile, it is  $t = 300$  s at position  $z = 10$  m. These two times are exactly the same with that time for loose seabed soil to become fully or partially liquefied at  $z = 18.5$  m and  $z = 10$  m. This kind of coincidence would remind us that the phenomenon that residual stress angle from increasing to keeping stable could be adopted as another indirect indicator to judge the occurrence of soil liquefaction.

Due to the build up of pore pressure in seabed under wave loading, there is a upward pore pressure gradient (seepage force) formed in the upper seabed. It directly results in the upward movement of pore water, finally draining out through seabed surface from seabed to seawater. This process is the pore pressure dissipation. Therefore, the build up and dissipation of pore pressure both exist simultaneously in seabed under cyclic loading. Before the occurrence of liquefaction, the speed of pore pressure build up is generally greater than that of pore pressure dissipation. After liquefaction, residual pore pressure will basically keep stable if pore pressure build up is balanced with pore pressure dissipation; while residual pore pressure will gradually reduce if pore pressure dissipation is dominant. Fig. 5 quantitatively illustrates the discharging velocity  $q$  and accumulative volume  $Q$  of pore water draining out from seabed surface. It is shown that the discharging velocity  $q$  is always positive value, meaning that pore water always draining out from loose seabed before  $t = 500$  s. After that, there are a great number of negative value for discharging velocity  $q$ , meaning that pore water also can go into loose seabed from seawater at some times under wave loading. This result clearly proves that there is fluid

exchange between seawater and pore water in loose seabed. However, some pore water is finally drained out from seabed surface as a whole. In Fig. 5, it is shown that nearly 9L pore water is finally drained out through  $1 \text{ m}^2$  seabed surface.

Distribution of dynamic pore pressure and effective stress can further improve our understanding on the response characteristics of loose seabed floor to wave & current. As illustrated in Fig. 6, the wave & current-induced pore pressure in loose seabed floor is not uniform, but wavy in upper seabed. It is indicated that the dynamics of upper seabed is significantly affected by ocean wave. With time passing from  $t/T=25$  to  $t/T = 50$ , the distribution of dynamic pore pressure and mean effective stress in the upper seabed basically has no change. However, the dynamic pore pressure in lower seabed has been build up significantly; meanwhile, the mean effective stress also has been reduced correspondingly.

## 5.2. Displacement

Previous investigation have proved that liquefied soil behaves like a kind of heavy fluid. In the above analysis, it has been known that the upper loose seabed soil become liquefied under continuous wave & current loading. Then, with the overlying sea water, a two-layer fluid system is formed. Under wave & current loading, the liquefied seabed soil is supposed to vibrate driven by the overlying wave & current motion. The wave & current-induced displacement of seabed at  $z = 18.5$  m is demonstrated in Fig. 7. It is observed that there is obvious lateral spreading in the loose seabed soil, especially after soil liquefaction. At  $t = 450$  s, lateral spreading reaches nearly 80 cm. Additionally, there is also significant vertical subsidence (reaching about 8 cm) in the loose seabed accompanying pore water drainage out of seabed surface.

The most important characteristics of vertical displacement is that its amplitude is gradually increasing under wave & current loading. Before seabed soil become liquefied, the amplitude of vertical displacement is less. After liquefaction, its amplitude gradually increases due to the fact that the wave & current-induced liquefaction zone in loose seabed becomes larger and larger. Actually, this is a kind of resonance phenomenon in the two-layer fluid system driven by the overlying wave & current motion. This resonance phenomenon also has been observed in a series of wave flume tests in laboratory (Sassa and Sekiguchi, 1999; Wang et al., 2014; Kirca et al., 2013). It is indicated that the developed model FSSI-CAS 2D incorporating PZIII soil model is reliable to understand the dynamic response of offshore loosely deposited seabed soil under hydrodynamic loading.

## 5.3. Progressive liquefaction

It has been widely verified that loose seabed soil could liquefy under ocean hydrodynamic loading by laboratory tests (Sassa and Sekiguchi, 1999) and field records (Sassa et al., 2006). There are, generally, two types of liquefaction mechanisms for seabed soil. One is momentary liquefaction, only occurring in very dense sand under wave trough. Its effect on the transient stability of offshore structures is minor. However, momentary liquefaction could boost the scouring of seabed soil around offshore structures. Another is residual liquefaction due to pore pressure build up in loose soil. The liquefaction occurring in offshore loose seabed soil in this study is exactly the residual liquefaction. Generally, residual liquefaction in seabed foundation has fatal effect on the stability of offshore structures. Once residual liquefaction occurs in seabed soil, bearing capacity of seabed soil will basically completely lost.

In this study, a parameter named residual liquefaction potential  $L_{potential}$  is defined to describe the liquefaction characteristics of loose seabed under wave & current loading:

$$L_{potential} = \frac{\sigma'_{zd}}{-\sigma'_{z0} + \alpha c} \quad (11)$$

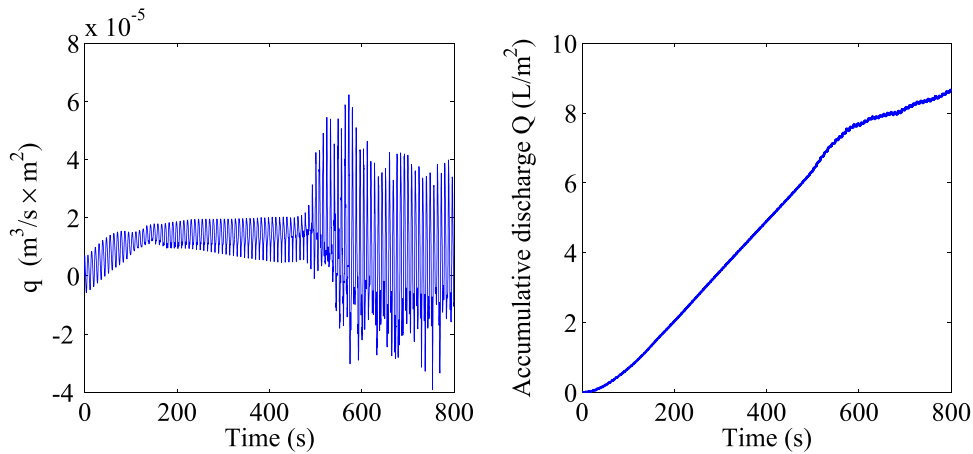


Fig. 5. Time history of velocity  $q$  and accumulative volume  $Q$  of pore water draining out from seabed surface.

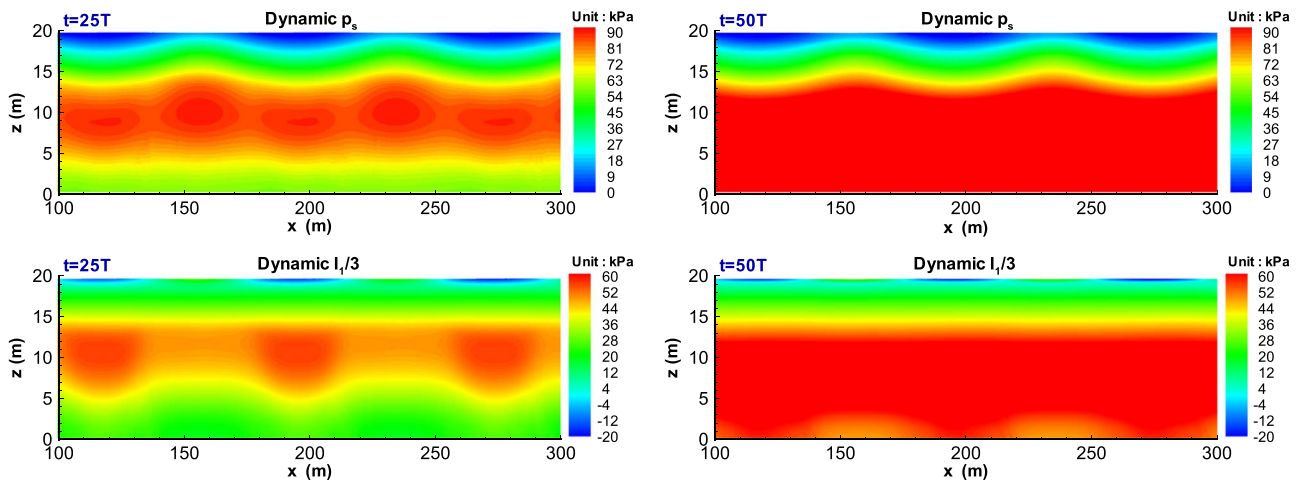


Fig. 6. Distribution of wave & current-induced dynamic pore pressure and mean effective stress in loose seabed floor at time  $t/T = 25$  and  $t/T = 50$ .

where  $\sigma'_{zd} = \sigma'_z - \sigma'_0$  is wave-induced dynamic vertical effective stress;  $\sigma'_0$  is initial vertical effective stress;  $\sigma'_z$  is current vertical effective stress.  $c$  is cohesion of seabed soil;  $\alpha$  is a material coefficient. In Eq. (11), the cohesion of seabed soil is considered. From the point of review that cohesive soil is much more difficult to become liquefied under cyclic loading, it is indicated that cohesion of soil could effectively boost the liquefaction resistance of soil  $L_r = -\sigma'_{z0} + \alpha c$  (Liu and Jeng, 2016). Therefore, cohesion  $c$  of soil must be considered when defining liquefaction potential. Due to the fact that macroscopic cohesion  $c$  of soil is not absolutely equivalent to microscopic liquefaction resistance

of soil particles, a material coefficient must be added to cohesion  $c$  of soil in Eq. (11). Currently, investigation on the effect of cohesion of soil on its liquefaction resistance is limited. As a result, the value of material coefficient  $\alpha$  is not sure. This will be an interesting topic in the future. In this study, cohesion  $c$  is zero because seabed is assumed to be sandy soil. Then, there is no effect of  $\alpha$  on  $L_{potential}$  of sandy seabed soil. However,  $\alpha$  must be quantitatively determined based on laboratory test for silty soil and cohesive soil when evaluating their liquefaction potential under cyclic loading.

In theory, when  $L_{potential}$  is greater than or equal to 1.0, sandy soil

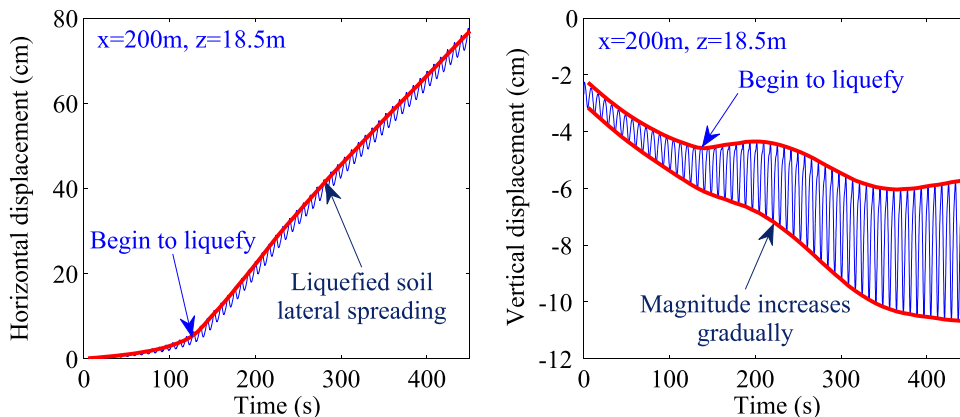


Fig. 7. Time history of wave & current-induced displacement of seabed at  $z = 18.5$ . It is shown that liquefied seabed soil has significant lateral spreading and vertical vibration driven by ocean wave.

becomes liquefied. But actually,  $L_{potential}$  of sandy soil will not exceed 1.0 either in numerical computation or in laboratory tests (Ishihara, 1993; Wu et al., 2004). The reason is that sandy soil is non-cohesive granular material. It can not bear any tensile stress as silty and cohesive soil. There is no yield surface and plastic potential surface in the tension stress space. Therefore, sandy seabed soil is difficult to reach fully liquefied status ( $L_{potential} = 1.0$ ) in numerical computation. In laboratory tests, this phenomenon is also observed, for instance, Ishihara (1993) found that  $L_{potential}$  in silty sands or sandy silts containing some amount of fines stopped to build up when it has reached to about 0.9 to 0.95. If liquefaction was strictly defined as the occurrence of  $L_{potential} = 1.0$ , then seabed soils would never “liquefy” despite of the fact that they may have behaved as liquefiable materials. Some laboratory soil tests (Wu et al., 2004; Kammerer et al., 2002; Wu et al., 2003) performed at U.C. Berkeley also shown that liquefaction still could occur when the residual excess pore pressure did not reach the downward initial vertical effective stress, namely when  $L_{potential} < 1$ . Here, this liquefaction is referred as to partial liquefaction. Based on the above recognition, it is defined that seabed sandy soil will liquefy if the  $L_{potential} \geq \alpha_r$ , in which  $\alpha_r$  is also a coefficient depending on the soil characteristics. Its range generally is 0.78-0.99 (Wu et al., 2004). Based on previous investigation,  $\alpha_r$  is determined as 0.86 for the loose seabed soil in this study (Ye et al., 2015).

The essence of residual soil liquefaction in loose seabed is the build-up of residual pore pressure under hydrodynamic loading. When excess residual pore pressure is equal to or greater than the initial contact effective stress between soil particles, sandy soil become liquefied. It is highly necessary for us to understand the vertical distribution characteristics of residual pore pressure under wave & current loading. In Fig. 8, this vertical distribution characteristics of residual pore pressure, as well as oscillatory pore pressure at different times on  $x = 200$  m are shown. It is clearly observed that residual pore pressure in loose seabed continuously builds up with time. However, there is a limitation line to constrain the build-up of residual pore pressure. Residual pore pressure can not exceed this limitation line. Actually, this limitation line is the above mentioned liquefaction resistance line (LRL). When wave & current-induced residual pore pressure reaches to LRL at a depth, the seabed soil at this depth becomes liquefied. According to Eq. (11), liquefaction potential  $L_{potential}$  along depth in loose seabed floor at typical times  $t/T = 10, 25, 50, 100$  are estimated respectively, as demonstrated in Fig. 9. It is clearly found that  $L_{potential}$  in upper seabed is generally greater than that in lower seabed at any time; and  $L_{potential}$  in whole seabed gradually increases to  $\alpha_r$  with wave & current loading. Once  $L_{potential}$  becomes greater than  $\alpha_r$  at a depth, it means seabed soil becomes liquefied at this depth. Then  $L_{potential}$  at this depth will not significantly increase. Overall, there is no a depth where

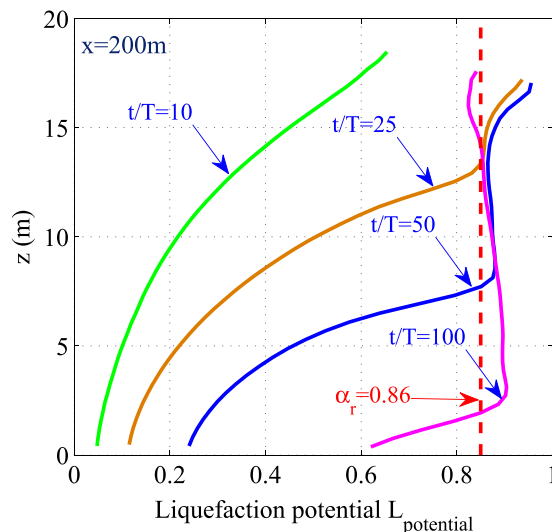


Fig. 9. Vertical distribution of liquefaction potential  $L_{potential}$  at typical time  $t/T = 10, 25, 50, 100$ .

$L_{potential}$  could reach 1.0 (its reason has been analyzed above).

Figs. 8 and 9 both show that the time needed for residual pore pressure reaching LRL is positively related to buried depth of seabed soil. It means that hydrodynamic loading-induced liquefaction in loose seabed is a progressive process, initiating at surface, and gradually propagating downward, as illustrated in Fig. 10. After  $t/T = 100$ , the residual liquefaction depth is about 18 m.

The vertical distribution of oscillatory pore pressure on  $x = 200$  m also owns interesting characteristics. It is found that oscillatory pore pressure in loose seabed is significantly greater than that in dense seabed. It is also observed that the vertical distribution of oscillatory pore pressure is oscillatory in upper liquefied seabed soil; while, it is regular in lower non-liquefied seabed soil. This typical vertical distribution characteristics of oscillatory pore pressure could also be taken as an indirect indicator to predict the depth of residual liquefaction in numerical computation in the future.

Stress path is another important way to characterise the wave & current-induced liquefaction in loose seabed floor. Fig. 11 demonstrates a series of stress paths at several typical positions on  $x = 200$  m. It is found that all stress states at initial time are located on initial  $K_0$  line. Under wave & current continuous loading, effective stress in loose seabed reduces resulting from the build-up of pore pressure. As a result, the stress state gradually moves toward to the zero stress state (namely liquefaction state). At the end of computation, the stress state

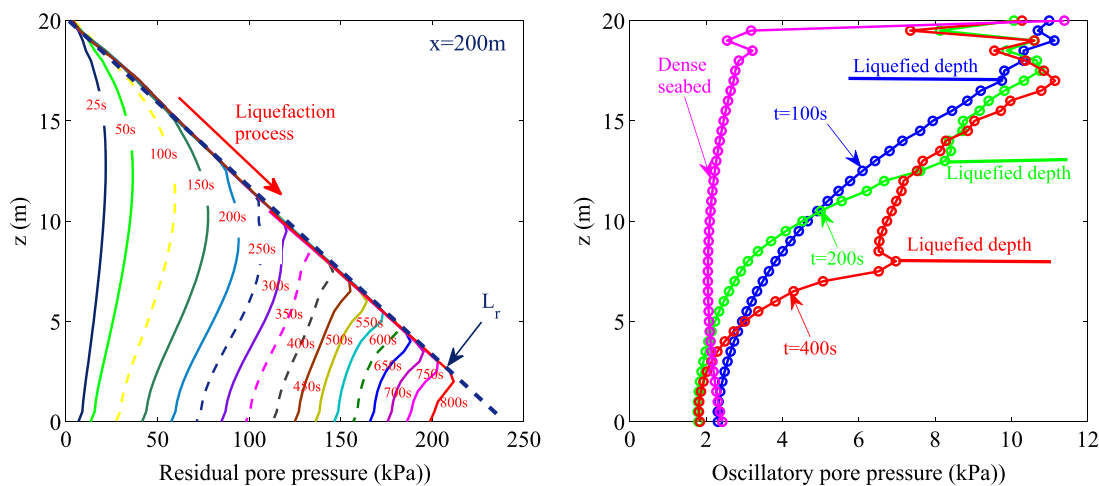


Fig. 8. Vertical distribution of wave & current-induced residual pore pressure and oscillatory pore pressure on symmetrical line  $x = 200$  m.

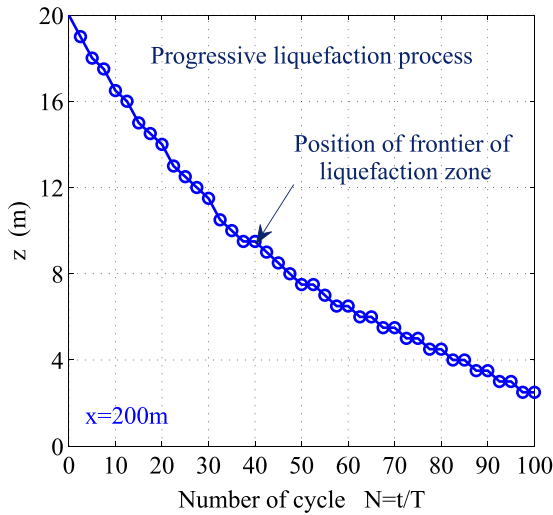


Fig. 10. Position of the frontier of residual liquefaction zone on  $x = 200$  m, showing the progressive liquefaction process in loose seabed floor under wave & current loading.

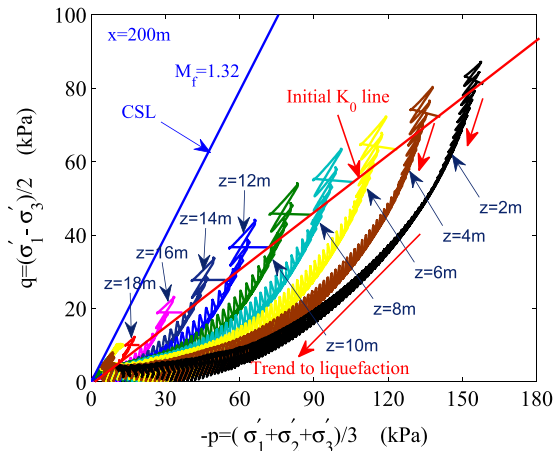


Fig. 11. Wave & current-induced stress paths at a series of positions on  $x = 200$  m.

at a series of positions on  $x = 200$  m has reached or approached the zero stress state, becoming fully or partially liquefied.

Liquefaction zone shown in Fig. 12 is predicted based on the definition of liquefaction potential  $L_{potential}$ . When  $L_{potential} \geq 0.86$  at a position, it is predicted that seabed soil here become liquefied. In

Fig. 12, it is observed that the liquefaction zone in loose seabed floor gradually enlarges with time. The shape of liquefaction zone frontier is wavy affected by the motion of ocean wave. To  $t/T = 100$ , most of the loose seabed floor become liquefied (liquefaction depth reaches 18 m as analyzed above).

5.4. Stress-strain relation

Dynamic response of loose seabed to wave & current has shown some nonlinear characteristics in the above analysis. Stress-strain relations demonstrated in Fig. 13 further prove the nonlinearity of dynamics of loose seabed soil to wave & current. In Fig. 13, it is observed that there is cyclic mobility at all depths in loose seabed under wave & current loading. The mobility speed is relatively slow in early stage; it will accelerate significantly in later stage. At the end of computation, shear strain at  $(x = 200\text{m}, z = 18.5\text{ m})$  in upper seabed is as huge as 60%, meaning that there is significant lateral spreading after partial liquefaction in upper seabed under wave & current loading. However, it is only 0.2 % at  $(x = 200\text{ m}, z=2\text{ m})$ . It is indicated that the magnitude of shear strain is negatively related to buried depth, even though shear stress is positively related to buried depth. From the relation of  $\tau_{xz}-\epsilon_v$ , it is found that loose seabed soil are all contractive under hydrodynamic loading; and the magnitude of contraction has negative relation with buried depth. The contraction of seabed soil under hydrodynamic loading represents that there is pore water being drained out from the surface of seabed in the process of wave & current loading, as demonstrated in Fig. 5.

5.5. Parametric study

Effect on wave characteristics (wave height, period, water depth and current velocity) and soil characteristics (permeability and saturation) on the progressive liquefaction process in loose seabed under wave & current loading are illustrated in Figs. 14 and 15, respectively. In Fig. 14, it is obviously found that effect of wave height  $H$  is most significant; and the effect of water depth  $d$  and current velocity  $U$  is not important. In general, co-flow ( $U_0 > 0$ ) makes the liquefaction process faster; whereas inverse flow ( $U_0 < 0$ ) makes the liquefaction process slower. However, the dynamics of loose seabed to wave & current is similar with each other, regardless of co-flow, inverse flow or without flow. The only difference is the magnitude, speed of seabed dynamics to wave & current. After 75 cycles of wave & current loading, the liquefaction depth reaches 20 m for the case  $H = 4.0\text{ m}$ ; while it is only 11 m if  $H = 2.0\text{ m}$ . Their difference is significant. Overall, wave & current-induced liquefaction depth in loose seabed floor is positively

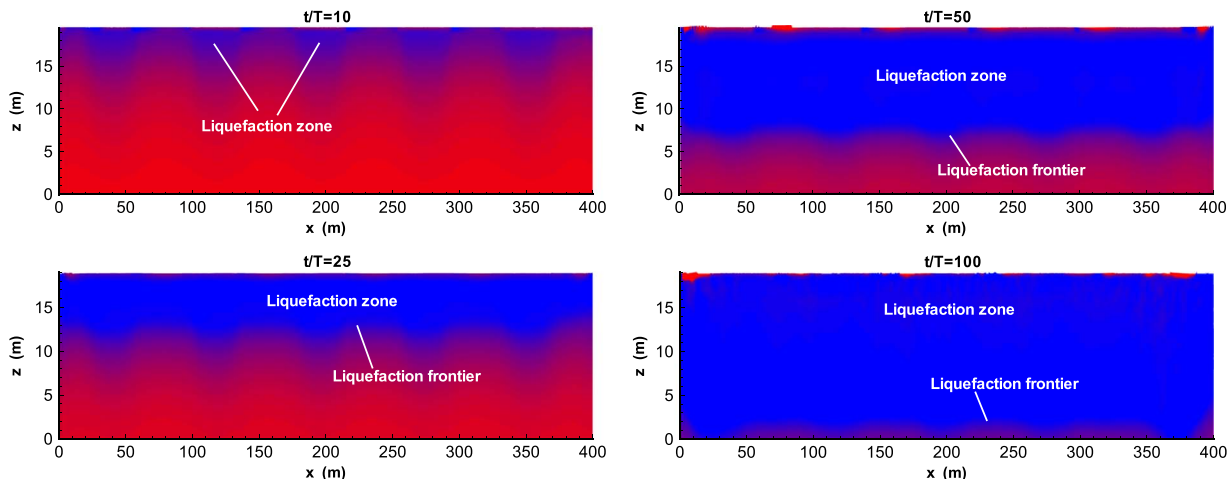


Fig. 12. Wave & current-induced residual liquefaction zone in loose seabed floor at typical time  $t/T = 10, 25, 50, 100$  (It is noted that zone with blue color present the liquefaction zone).

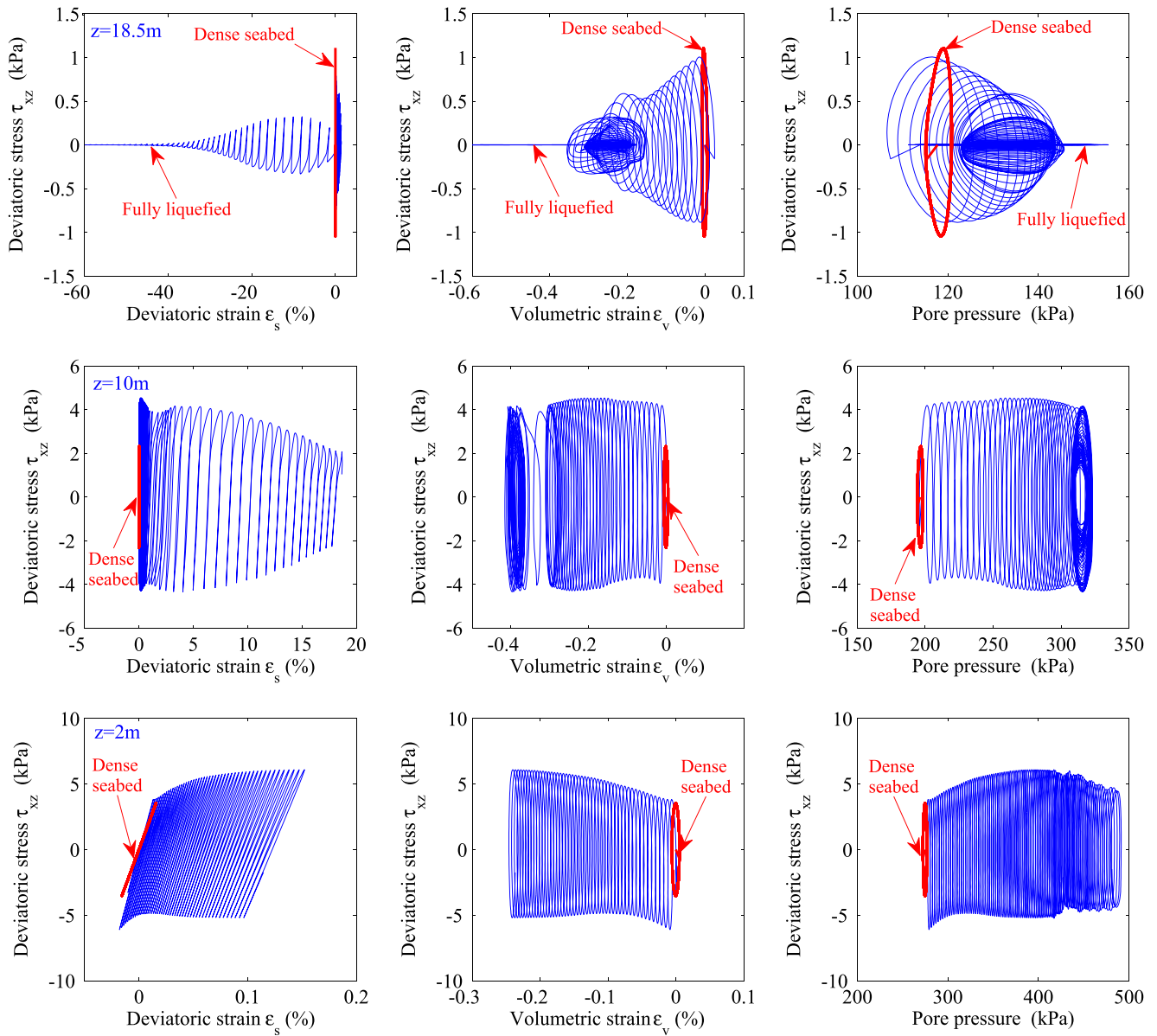


Fig. 13. Stress-strain relation at three typical positions on  $x = 200$  m.

related to wave height, wave period and current velocity; and negatively related to water depth.

In Fig. 15, it is observed that permeability and saturation of soil both could significantly affect the progressive liquefaction process. It is shown that there is no liquefaction occurring in loose seabed if permeability  $k$  is not less than  $1.0 \times 10^{-2}$  m/s. Overall, liquefaction depth is negatively related to permeability. However, its effect basically disappears when permeability less than  $1.0 \times 10^{-5}$  m/s. It is indicated that the effect of permeability of soil to residual liquefaction process owns range limitation. Finally, for loose seabed floor, wave & current-induced liquefaction depth is positively related to saturation of soil.

## 6. Conclusion

Quaternary newly deposited loose seabed soil widely distributes in offshore area in the world. Wave-induced residual liquefaction in loose seabed floor brings great risk to the stability of offshore structures in extreme climate. The understanding of the characteristics of wave-induced residual liquefaction in loose seabed is meaningful for engineers involved in design of offshore structures. In this study,

wave & current-induced residual liquefaction has been investigated deeply and comprehensively adopting a validated integrated numerical model. It is shown that the integrated numerical model FSSI-CAS 2D incorporating PZIII soil model can effectively and precisely capture a series of nonlinear dynamic response characteristics of loose seabed floor under wave & current loading. The computational results further confirm the wave-induced liquefaction in loose seabed soil is progressively downward, initiating at seabed surface. Besides, it is found that three physical processes, including vertical distribution of oscillatory pore pressure, time history of stress angle, as well as lateral pressure coefficient  $K_0$  could be taken as indirect indicator to judge the occurrence of wave-induced residual liquefaction, or to predict the depth of residual liquefaction in loose seabed. It is also found that the progressive liquefaction process is significantly affected by wave height, permeability and saturation of seabed soil. Finally, the classic effective stress principle has been modified to describe the nonlinear phenomenon that the reduction rate of vertical effective stress  $\sigma'_z$  is faster than that of horizontal effective stress  $\sigma'_x$  and  $\sigma'_y$  accompanying residual pore pressure building up.

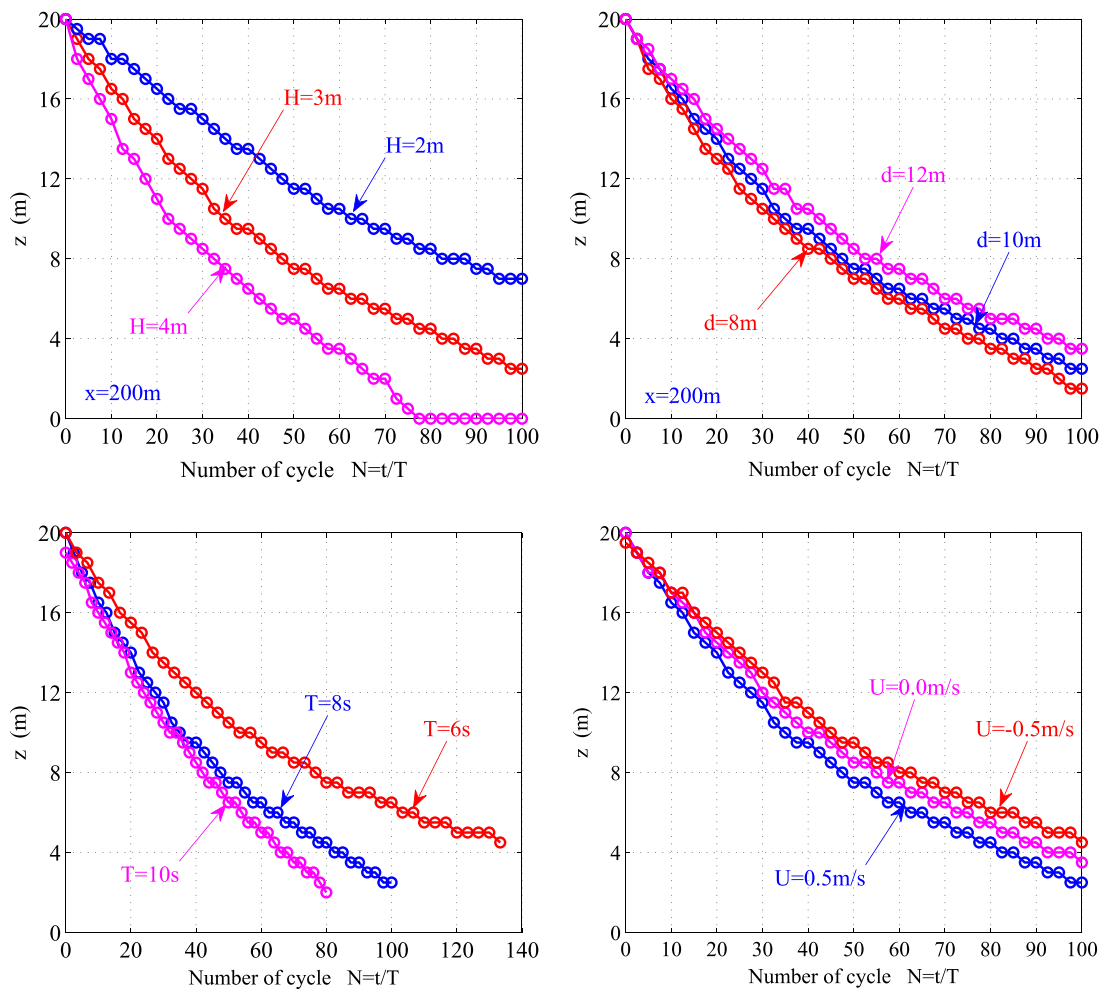


Fig. 14. Effect of wave characteristics on the progressive liquefaction process in loose seabed floor under wave & current loading.

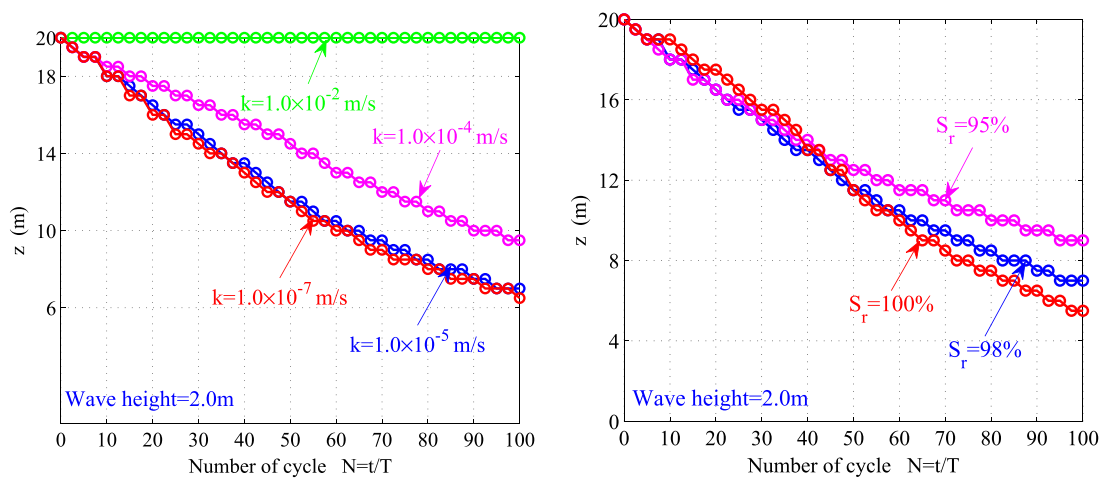


Fig. 15. Effect of soil characteristics on the progressive liquefaction process in loose seabed floor under wave & current loading.

**Acknowledgements**

Dr Guoxiang Yang thanks for the funding support from National Natural Science Foundation of China under project 41302234 as well as Fundamental Research Funds for the Central Universities, China. Professor Jianhong YE are also grateful to the funding support from National Natural Science Foundation of China under project 41472291.

**References**

Chan, A.H.C., 1988. A unified finite element solution to static and dynamic problems of geomechanics. PhD thesis, University of Wales, Swansea Wales.  
 Chang, S.C., Chien, L.K., Lin, J.G., Chiu, Y.F., 2007. An experimental study on progressive wave-induced stresses duration in seabed soil. *J. Mar. Sci. Technol.* 15 (2), 129–140.  
 Cheng, L., Sumer, B.M., Fredsoe, J., 2001. Solution of pore pressure build up due to progressive waves. *Int. J. Numer. Anal. Method Geomech.* 25 (9), 885–907.  
 Dunn, S.L., Vun, P.L., Chan, A.H.C., Damgaard, J.S., 2006. Numerical modeling of wave-

- induced liquefaction around pipelines. *J. Waterw. Port Coast. Ocean Eng.* 132 (4), 276–288.
- Hsu, J.R., Jeng, D.S., 1994. Wave-induced soil response in an unsaturated anisotropic seabed of finite thickness. *Int. J. Numer. Anal. Methods Geomech.* 18 (11), 785–807.
- Hsu, T.J., Sakakiyama, T., Liu, P.L.F., 2002. A numerical model for wave motions and turbulence flows in front of a composite breakwater. *Coast. Eng.* 46, 25–50.
- Ishihara, K., 1993. Liquefaction and flow failure during earthquakes. *Géotechnique* 43 (3), 351–451.
- Jeng, D.S., Hsu, J.R.C., 1996. Wave-induced soil response in a nearly saturated seabed of finite thickness. *Géotechnique* 46 (3), 427–440.
- Jeng, D.S., Ou, J., 2010. 3d models for wave-induced pore pressures near breakwater heads. *Acta Mech.* 215 (1–4), 85–104.
- Jeng, D.S., Zhao, H.Y., 2015. Two-dimensional model for accumulation of pore pressure in marine sediments. *J. Waterw. Port Coast. Ocean Eng.* 141 (3).
- Jeng, D.-S., 2003. Wave-induced sea floor dynamics. *Appl. Mech. Rev.* 56 (4), 407–429.
- Kammerer, A.M., Pestana, J.M., Seed, R.B., 2002. Undrained response of monterey 0/30 sand under multidirectional cyclic simple shear loading conditions. Technical report, University of California, Berkeley. Geotechnical Engineering Research Report No. UCB/GT/02-01.
- Kirca, V., Sumer, B., Fredsoe, J., 2013. Residual liquefaction of seabed under standing waves. *J. Waterw. Port Coast. Ocean Eng.* 139 (6), 489–501.
- Lee, T.C., Tsai, C.P., Jeng, D.S., 2002. Ocean wave propagating over a porous seabed of finite thickness. *Ocean Eng.* 29, 1577–1601.
- Li, J., Jeng, D.S., 2008. Response of a porous seabed around breakwater heads. *Ocean Eng.* 35 (8–9), 864–886.
- Liao, C.C., Jeng, D.S., Zhang, L.L., 2015a. An analytical approximation for dynamic soil response of a porous seabed due to combined wave and current loading. *J. Coast. Res.* 31 (5), 1120–1128.
- Liao, C.C., Zhao, H., Jeng, D.S., 2015b. Poro-elasto-plastic model for the wave-induced liquefaction. *J. Offshore Mech. Arctic Eng.* 137 (4), 042001.
- Liu, Z., Jeng, D.-S., Chan, A.H.C., Luan, M., 2009. Wave-induced progressive liquefaction in a poro-elastoplastic seabed: A two-layered model. *Int. J. Numer. Anal. Methods Geomech.* 33 (5), 591–610.
- Liu, B., Jeng, D.S., 2016. Laboratory study for influence of clay content (cc) on wave-induced liquefaction in marine sediments. *Marine Georesources and Geotechnology*, In press: <http://dx.doi.org/10.1080/1064119X.2015.1005322>.
- Lu, X., Cui, P., 2004. The liquefaction and displacement of highly saturated sand under water pressure oscillation. *Ocean Eng.* 31 (7), 795–811.
- Lu, H.B., 2005. The research on pore water pressure response to waves in sandy seabed. Master's thesis, Changsha University of Science & Technology, Changsha, Hunan China.
- Madsen, O.S., 1978. Wave-induced pore pressure and effective stresses in a porous bed. *Géotechnique* 28 (4), 377–393.
- Miyamoto, J., Sassa, S., Sekiguchi, H., 2004. Progressive solidification of a liquefied sand layer during continued wave loading. *Géotechnique* 54 (10), 617–629.
- Mizutani, N., Mostarfa, A., Iwata, K., 1998. Nonlinear regular wave, submerged breakwater and seabed dynamic interaction. *Coast. Eng.* 33, 177–202.
- Mostafa, A., Mizutani, N., Iwata, K., 1999. Nonlinear wave, composite breakwater, and seabed dynamic interaction. *J. Waterw. Port Coast. Ocean Eng. ASCE* 25 (2), 88–97.
- Oka, F., Yashima, A., Shibata, T., Kato, M., Uzuoka, R., 1994. Fem-fdm coupled liquefaction analysis of a porous soil using an elasto-plastic model. *Appl. Sci. Res.* 52 (3), 209–245.
- Ou, J., 2009. Three-dimensional numerical modelling of interaction between soil and pore fluid. PhD thesis, University of Birmingham, Birmingham, UK.
- Pastor, M., Zienkiewicz, O.C., Chan, A.H.C., 1990. Generalized plasticity and the modelling of soil behaviour. *Int. J. Numer. Anal. Methods Geomech.* 14, 151–190.
- Pastor, M., Chan, A.H.C., Mira, P., Manzanal, D., Fernández, M.J.A., Blanc, T., 2011. Computational geomechanics: the heritage of olek zienkiewicz. *Int. J. Numer. Methods Eng.* 87 (1–5), 457–489.
- Rahman, M.S., Jaber, W.Y., 1986. Simplified drained analysis for wave-induced liquefaction in ocean floor sands. *Soils Found.* 26 (3), 57–68.
- Sassa, S., Sekiguchi, H., 1999. Wave-induced liquefaction of beds of sand in a centrifuge. *Géotechnique* 49 (5), 621–638.
- Sassa, S., Sekiguchi, H., Miyamoto, J., 2001. Analysis of progressive liquefaction as a moving-boundary problem. *Géotechnique* 51 (10), 847–857.
- Sassa, S., Takayama, T., Mizutani, M., Tsujio, D., 2006. Field observations of the build-up and dissipation of residual porewater pressures in seabed sands under the passage of stormwaves. *J. Coast. Res.* 39, 410–414.
- Seed, H.B., Rahman, M.S., 1978. Wave-induced pore pressure in relation to ocean floor stability of cohesionless soils. *Mar. Geotechnol.* 3 (2), 123–150.
- Seed, H.B., Martin, P.O., Lysmer, J., 1976. Pore-water pressure changes during soil liquefaction. *J. Geotech. Eng. ASCE* 102 (4), 323–346.
- Sumer, M.B., Hatipoglu, F., Fredsoe, J., Kaan, S.S., 2006. The sequence of sediment behaviour during wave-induced liquefaction. *Sedimentology* 53 (3), 611–629.
- Summer, B.M., Dixen, F.H., Fredsoe, J., 2010. Cover stones on liquefiable soil bed under waves. *Coast. Eng.* 57, 864–873.
- Teh, T.C., Palmer, A.C., Damgaard, J.S., 2003. Experimental study of marine pipelines on unstable and liquefied seabed. *Coast. Eng.* 50 (1–2), 1–17.
- Tsai, C.P., Lee, T.L., 1995. Standing wave induced pore pressure in a porous seabed. *Ocean Eng.* 22 (6), 505–517.
- Wang, H., Liu, H.J., Zhang, M.S., 2014. Pore pressure response of seabed in standing waves and its mechanism. *Coast. Eng.* 91, 213–219.
- Wu, J., Kammerer, A.M., Riemer, M.F., Seed, R.B., Pestana, J.M., 2004. Laboratory study of liquefaction triggering criteria. In Proceedings of 13th World Conference on Earthquake Engineering, Vancouver, British Columbia, Canada. Paper No. 2580.
- Wu, J., Seed, R.B., Pestana, J.M., 2003. Liquefaction triggering and post liquefaction deformations of monterey 0/30 sand under uni-directional cyclic simple shear loading. Technical report, University of California, Berkeley. Geotechnical Engineering Research Report No. UCB/GE-2003/01.
- Xu, H., Dong, P., 2011. A probabilistic analysis of random wave-induced liquefaction. *Ocean Eng.* 38 (7), 860–867.
- Yamamoto, T., Koning, H., Sellmeijer, H., Hijum, E.V., 1978. On the response of a poro-elastic bed to water waves. *J. Fluid Mech.* 87 (1), 193–206.
- Ye, J.H., 2012b. Numerical modelling of consolidation of 2-D porous unsaturated seabed under a composite breakwater. *Mechanika* 18 (4), 373–379.
- Ye, J.H., Jeng, D.S., 2012. Response of porous seabed to nature loadings: waves and currents. *J. Eng. Mech. ASCE* 138 (6), 601–613.
- Ye, J.H., Wang, G., 2015. Seismic dynamics of offshore breakwater on liquefiable seabed foundation. *Soil Dyn. Earthq. Eng.* 76, 86–99.
- Ye, J.H., Jeng, D.-S., Wang, R., Zhu, C.-Q., 2013. Validation of a 2D semi-coupled numerical model for Fluid-Structures-Seabed Interaction. *J. Fluids Struct.* 42, 333–357.
- Ye, J.H., Jeng, D.-S., Wang, R., Zhu, C.-Q., 2015. Numerical simulation of wave-induced dynamic response of poro-elasto-plastic seabed foundation and composite breakwater. *Appl. Math. Model.* 39, 322–347.
- Ye, J.H., 2012a. Numerical analysis of wave-seabed-breakwater interactions. PhD thesis, University of Dundee, Dundee, UK.
- Zhou, X.L., Wang, J.H., Xu, B., Li, Y.L., 2013. An analytical solution for wave-induced seabed response in a multi-layered poroelastic seabed. *Ocean Eng.* 38 (1), 119–129.
- Zienkiewicz, O.C., Chang, C.T., Bettess, P., 1980. Drained, undrained, consolidating and dynamic behaviour assumptions in soils. *Géotechnique* 30 (4), 385–395.
- Zienkiewicz, O.C., Chan, A.H.C., Pastor, M., Schrefler, B.A., Shiomi, T., 1999. *Computational Geomechanics with Special Reference to Earthquake Engineering*. John Wiley and Sons, England.
- Zienkiewicz, O.C., Mroz, Z., 1984. Generalized plasticity formulation and applications to geomechanics. In *Mechanics of Engineering Materials*. Chichester: John, Cambridge UK.